

Study on Selection of Diesel Engine Exhaust After-Treatment System Materials and Emission Performance for GenSet Applications

Karthikeyan Subramanian^{1*} and Annamalai Kandaswamy²

0000-0002-7905-0021, 0000-0002-8950-3645

¹Exhaust and After-Treatment System Department, Ashokleyland Technical Centre, TamilNadu, Chennai, 600103, India

²Automobile Engineering Department, M.I.T Campus, Anna University, TamilNadu, Chennai, 600044, India

Abstract

Due to the usage of off-road engines for a variety of applications, the contributions of their emission levels also increased, as do those of on-road engines. Therefore, the need for off-road engine emission reduction is essential. To overcome the aforementioned concern, it is a must to have clean diesel technologies such as Fuel Injection Equipment (FIE), Turbocharger with Intercooler (TCIC), Cooled Exhaust Gas Recirculation (C-EGR), and after-treatment systems like Diesel Oxidation Catalyst (DOC), Selective Catalytic Reduction (SCR), and Diesel Particulate Filter (DPF). In this paper, during the conversion of a 15 kW naturally aspirated engine to a 27 kW TCIC engine, the after-treatment system configurations and their influence on emission reduction performance to meet the upcoming diesel engine emission norms are studied. Initially, emission testing is carried out with the DOC catalyst for three different Pt catalyst configurations. Following the testing, a 1.0-liter DOC with a catalyst loading of 1 g/cuft is selected. Furthermore, using the selected DOC specifications, the performance of 4.7-liter DPF volume with Pt catalyst and 3.7-liter SCR specifications with Zeolite catalyst is studied using GT-SUIT software simulation. The maximum soot mass limit of 8 gm is simulated for the selected 4.7-liter DPF based on this simulation study. Further, in order to improve DPF inlet gas temperature for soot regeneration, an advanced Nanox (7% YPSZ) coating is applied to the DOC outer shell (Nanox top coat layer of 460-480 microns) and tested. for heat retention performance with coating.

Keywords: After-treatment system, GenSet, DOC, DPF, SCR, Simulation

Research Article

<https://doi.org/10.30939/ijastech..1207224>

Received 22.11.2022

Revised 15.01.2023

Accepted 12.02.2023

* Corresponding author
Karthikeyan Subramanian
skarthikeyan@gmail.com
Address: Exhaust and After-Treatment
Department, Ashokleyland, Technical
Centre, TamilNadu, Chennai, India

1. Introduction

Diesel engines are used for a wide range of applications due to their lower fuel consumption when compared to spark-ignition engines [1, 2]. Even though the efficiency of these engines is currently at a high level, there are still possibilities for further improvements both in performance and emissions, specifically for cost-competitive applications like generators (GenSets) and tractors.

Table 1. Emission norms for GenSet.

Engine Power	CPCB II Norms (Current-2022)			CPCB IV Norms (Proposed -2023)		
	CO	NOx+HC	PM	CO	NOx+HC	PM
19<kW≤37	g/kWh			g/kWh		
	3.5	4.7	0.3	3.5	4.7	0.03

Typically, the associated concerns from the engine are higher particulate and NOx emissions, which cause environmental problems [3, 4]. In light of the foregoing, the Indian government regularly updates the exhaust emission level regulations for engines. In India, currently applicable emission norms for generator sets are based on Central Pollution Control Board (CPCB) II, and the proposed new norms will be CPCB IV. The current and proposed emission norms applicable for GENSET engines are shown in Table 1. The aim of this study is to select an optimized after-treatment system to meet the upcoming emission norms for GenSet applications. Further, considering the engine exhaust emission, temperature, and exhaust gas mass flow rate, these after-treatment system designs and catalyst loadings are fine-tuned. Based on this study, to meet the upcoming emission norms, depending on the engine power requirements, this approach can be utilized for selection and optimization of the catalyst loadings and the after-treatment systems.

2. Materials for after-treatment systems

2.1. Diesel oxidation catalyst (DOC) configurations

For DOC selection, substrate configuration plays a vital role for catalyst light-off to reduce HC and CO as well as generate NO₂. Compared to an uncoated substrate, the catalyst coating can improve the substrate heating time by as much as 40%. Further, for better emission conversion efficiency with standard substrate technology, the increase in catalyst amount increases the pressure drop. Hence, the challenge of improving this trade-off relationship exists with standard porosity (porosity of approximately 35%) substrates. However, with an advanced high porosity (approximately 48–50% after catalyst coating) cordierite substrate selection, the above-mentioned trade-off can be enhanced [3,4]. The porosity configuration for cordierite substrate is shown in Figure 1.

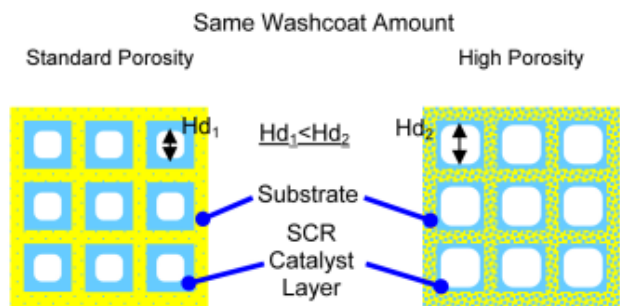


Fig. 1. Porosity configuration of cordierite substrate [5]

In a high-porosity substrate, the DOC catalyst penetrates the wall, and the catalyst amount on the wall surface is relatively small. As a result, in the high-porosity substrate fundamental concept, pores in the substrate walls are used as "added" catalyst support, suppressing decreases in hydraulic diameter (Hd) as the catalyst amount is increased [5–6]. Accordingly, selection of a substrate with thin wall technology is significant for increased open frontal area; for this, typically, cell densities of 300 and 400 cpsi for off-road diesel engines can be preferred. For this optimization study, the Pt catalyst with minimal zeolite catalyst is coated on the high porosity cordierite substrate with a mean pore size of 9.5–14.5 microns as well as wall porosity of 48–50%. Figure 2 shows the cordierite diesel oxidation systems developed for study.



Fig. 2. Cordierite diesel oxidation system

In addition, for these off-road applications, metallic substrates with advanced counter-corrugation techniques are also tested to compare the emission reduction performance. Figure 3 shows the metallic diesel oxidation systems developed for this study. The right-side image shows a metallic substrate, and the left-side image is a canned system.



Fig. 3. Metallic diesel oxidation system

This DOC system is installed before the DPF systems to generate NO₂ in the DPF for passive regeneration of soot. The NO₂ generation is explained in equation 1.



2.2. Selective Catalytic Reduction (SCR) configurations

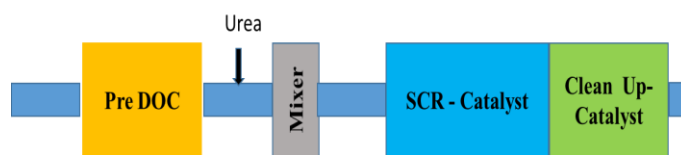
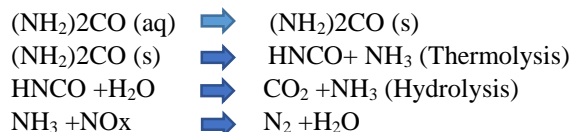


Fig. 4. SCR After-treatment system

Although a variety of SCR catalysts exist on the market, for this study, a zeolite-based catalyst with high porosity substrates was selected. Typically, with a suitable reducing agent and the existence of a catalyst, the nitrogen oxides emitted from the engine are reduced [7]. The reducing agent used in SCR applications is ammonia (NH₃), and urea solution is the most widely used. Urea-solution is eutectic with 32.5% urea and a balance of dematerialized water (by weight ratio), with the quality conforming to ISO 22241-1-2006. In the exhaust pipe, urea solution in the form of a fine spray is usually injected. During engine operation, when urea solution is injected, due to the high exhaust gas temperature, water evaporates, leaving urea (CO(NH₂)₂), which is further converted to ammonia via a two-step reaction mechanism. Urea decomposes into isocyanic (HNCO) acid due to heat (thermolysis). Isocyanic acid is an intermediate component [7, 8]. Iso-cyanic acid then reacts with water (hydrolysis) to form carbon dioxide and ammonia (NH₃). The SCR reactions are explained in the following equations:

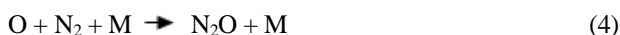


Overall, on the catalyst surface, the ammonia generated during the hydrolysis process reacts with the engine-out NO_x to form nitrogen and water [9]. The SCR after-treatment system is shown in Figure 4.

Furthermore, th-lee chemical reactions are important for this NO formation mechanism in the engine-out and are discussed below:



Equation 3 is an extended Zel'dovich mechanism. For the above-mentioned mechanism, the reaction rate is moderately slow as well as sensitive to temperature. Hence, thermal NO can appear in significant amounts only after the start of heat release, as it is influenced by temperature. Nitrous oxide (N₂O) is formed through a three-body mechanism at high pressures when oxygen atoms react with N₂.



M is used to remove energy from the above reaction in order to complete the reaction. It is a third body and molecule of another compound; otherwise, the energy released in a collision between the two reactants (O and N₂) would be sufficient to decompose back into the original reactants. Because of the additional molecule's presence, the energy release is absorbed by molecule M, which hence prevents the N₂O from decomposing. In addition, three-body reactions are also pressure-sensitive, and therefore, the significance of this reaction will increase at high pressures. Frequently, N₂O converts to N₂ through:



Nevertheless, under these conditions if the air-fuel ratio is lean, NO can form through the reaction:



The O in (6) comes from:



During the oxygen rich zone, due to the third body molecule interaction, O is formed. Hence, the N₂O third body reaction can be used to explain NO formation at lower temperatures as well as at higher pressures. Usually, NO represents around 90% of NO_x emissions, the remaining 10% is the most toxic NO₂. Nitrogen Dioxide (NO₂) is formed from Nitric Oxide (NO) by the below reaction:



When temperatures rise above those in the typical flame zone, Nitrogen Dioxide undergoes the following reaction:



During the low temperatures, unburnt fuel molecules can combine to form hydroperoxyl radicals (HO₂), which will be needed to form NO₂ as per equation 11.



Therefore, toxic NO₂ is formed as a by-product of thermal NO and also due to incomplete combustion of the fuel. However, using a diesel oxidation catalyst in the engine exhaust before the SCR catalyst increases the NO/NO₂ ratio. The diesel oxidation system plays a key role in NO₂ generation for facilitation of fast SCR reactions; this is mainly significant at low temperatures [9–10].

2.3. Diesel Particulate Filter (DPF) configurations

Typically, for a new DPF system, engine running-in (degreasing) conditions for the required temperature conditions are required, and a rapid rise in pressure drop begins during this period.

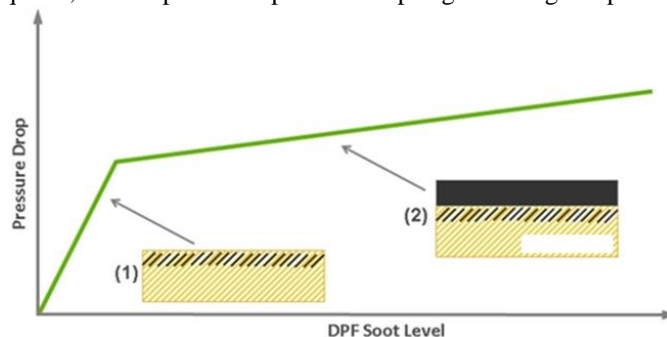


Fig. 5. Soot accumulation process

This is due to soot accumulation inside the filter pores (1), followed by a gradual increment in soot accumulation as a layer along the walls (2). Accordingly, DPF pressure drop increases with soot cake accumulation in the DPF. Soot particles are captured and retained in the DPF through an arrangement of depth filtration inside the filter pores and surface filtration along the channel walls. The aforementioned two processes of soot accumulation inside DPF are shown in Figure 5, where a small fraction of the soot initially accumulates in the filter pores (1) and then subsequently builds a layer along the channel walls (2). Hence, the soot filtration mechanisms play an important role in determining the overall increase in exhaust back pressure. If the accumulated soot regenerates without hydrocarbon dosing, then it is called a "passive regeneration process." For this, a platinum (Pt)-catalyst-coated DOC substrate is used to convert NO to NO₂ in the exhaust gas. In this study, for the selected catalyst, the passive regeneration of soot in the presence of NO₂ is accomplished between the temperature ranges of 250 °C and 375 °C [11–14]. Active regenerations are required due to the challenging operating conditions, and Cordierite DPF material is chosen to meet the DPF's robustness requirements. If the engine operates for a certain amount of time within this passive regeneration temperature window, then active regeneration may not be required. But for a prolonged period of time, if operated at a lower exhaust gas temperature of 250 °C, then active regeneration is desirable. Nevertheless, in the regeneration approach, the soot oxidation results in incombustible material, or ash, which cannot be burned and remains inside the DPF. Hence, it is critical to understand DPF pressure drop performance and select the size and volume of the cell structure for the filter accordingly. However, there are numerous DPF options available to meet the engine's application requirements. For this study, cordierite with 200 Cpsi cell densities and 12 mill-inch wall thicknesses were selected, as shown in Figure 6. The selected DPF for this study has an asymmetric cell configuration for more ash storage capacity as well as an increased ash cleaning interval. interval [15-16].

Material				 Monolithic design w/ low CTE approx. 10 ⁻⁷ /°C Cordierite & Aluminum Titanate material	
	Cordierite	Cordierite	Aluminum-Titanate		
	Bulk density	Low	Medium		High
	Pressure drop	Very low	Low		Low-Medium
	Soot mass limit	Low	Medium		High
Filtration	Very high	High	High/Very high	 ACT: Asymmetric Cell Technology for High Ash Storage	
	Low regen requirement system	Low regen requirement system			

Fig. 6. DPF selection parameters

Overall, using GT-Suite simulation software, the influence of selected DPF configurations considering the soot mass limit and backpressure performance as well as the time for completing the active regeneration and regeneration temperature conditions are studied in this paper.

2.4. Experimental Setup and Methodology

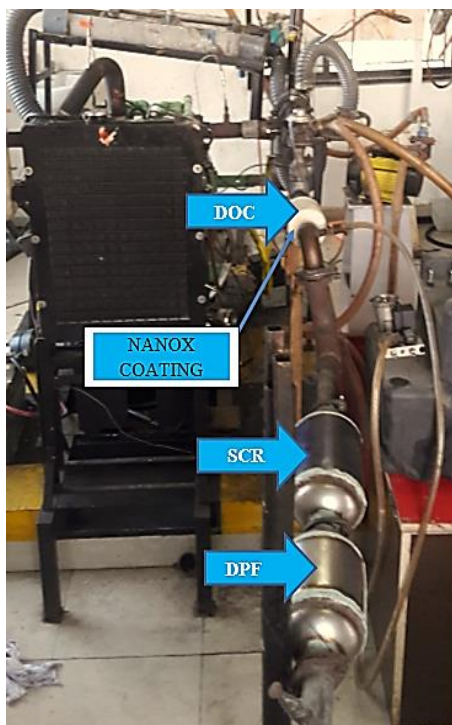


Fig. 7. After-treatment system experimental set-up coupled with engine

The after-treatment system experimental set-up coupled with the TCIC engine is shown in Figure 7. DOC is coated with a Nanox thermal barrier coating over the external surface for heat retention purposes. Further, downstream, after DOC, systems like SCR and DPF are installed. Initially, emission testing is carried out to optimize the DOC configuration. Based on the optimized DOC configuration, further SCR and DPF configurations are finalized based on GT-Simulation performance studies.

2.5. GT-SUITE Simulation

2.5.1. After-Treatment (DOC+SCR) modeling

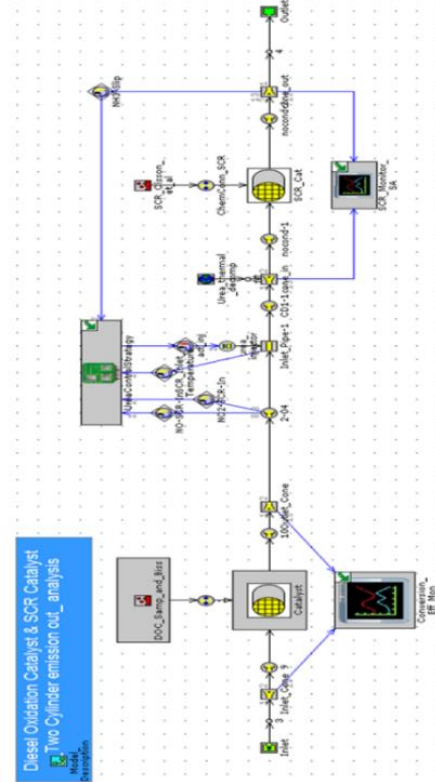


Fig. 8. DOC and SCR model for simulation

This simulation study was carried out to understand the emission conversion efficiency for the optimized DOC catalyst configuration and SCR system. In the first phase of simulation, the DOC model was only simulated to calibrate the ATS DOC model for simulation with reference to actual DOC testing results. The DOC catalyst-to-engine volume ratios of 0.35 (0.6-liter substrate volume), 0.47 (0.8 liter), and 0.58 (1.0 liter) are calibrated for GT-simulation. Using the previously calibrated DOC models, additional SCR system models were coupled together and simulated to assess NOx emission conversion efficiency [17]. The DOC and SCR discretized models coupled for GT-SUITE simulation are shown in Figure 8. With this model, HC, CO, and NOx emissions from the DOC outlet as well as NOx reduction efficiency from the SCR outlet are simulated. Furthermore, in this GT-Suite simulation, there are three flow solvers available for exhaust after-treatment models: explicit, implicit, and quasi-steady (QS). The QS solver is selected for all stand-alone exhaust after-treatment models due to its shorter computation time. However, the default time step size for the QS solver is 1 sec, which is used for this study. For this study, each test case runs for 1000 steps to stabilize, and the calculations are made accordingly. Due to generator applications for these constant speed engines, 5 mode cycle emission norms are used, and their emission weightage for each torque percent is shown in Table 2. The % emission conversion calculations for all five modes are based on this table, taking into account the emission weightage factors. Assumptions for simulation:

Table 2. Constant speed engine 5 mode weightage for emission

Torque %	100	75	50	25	10
Type D2	0.05	0.25	0.3	0.3	0.1

2.5.2. Diesel Particulate Filter Modeling

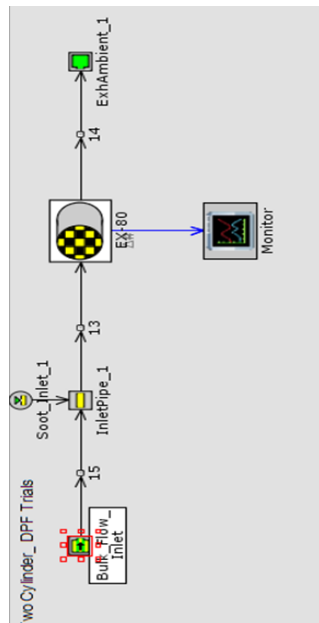


Fig. 9 (a). DPF soot generation model

For this study, DPF sizes of 3.4 and 3.7 liters are considered, and the DPF soot generation model developed for GT-SUITE simulation is shown in Figure 9 (a). Figure 9 (b) shows the pressure drop and DPF soot regeneration model used for this simulation. This diesel particulate filter model (wall flow type model) is accountable for filter pressure drop, soot loading, and full regeneration conditions, including ash creation. This DPF is a one- and zero-dimensional model, and it also assumes that the substrate temperature, gas phase temperature, pressure, and species compositions are identical throughout the filter wall along the channel. With the zero-dimensional model, it is assumed that particulate matter is oxidized inside the filter based on gaseous reactions. Accordingly, the filter temperature, soot mass, gas phase temperature, pressure, and species compositions are obtained by solving mass and energy equations for both the solid phase and gaseous phase.

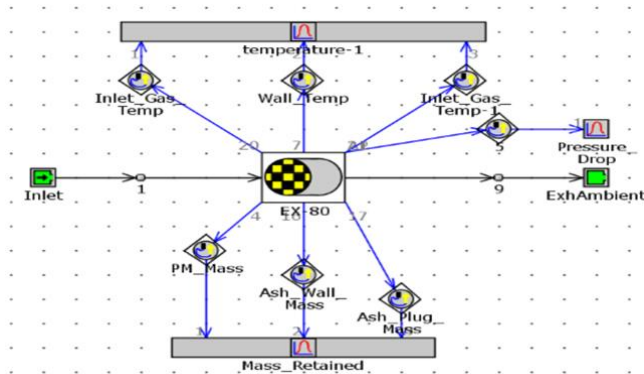


Fig. 9 (b). Pressure drop and DPF regeneration model

3. Results and discussion

Simulation results

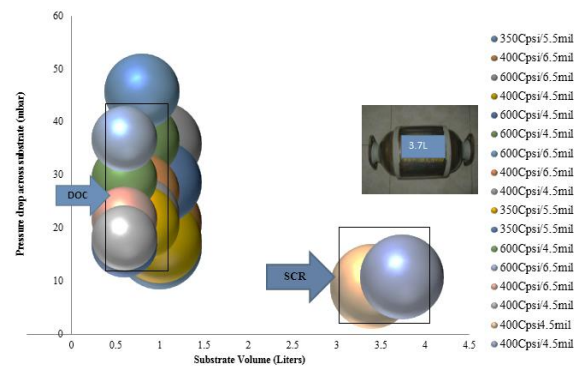


Fig. 10. Pressure drop simulation across DOC and SCR substrates

Figure 10 shows the pressure drop across DOC and SCR. For this study, various substrate volumes and cell densities of advanced high porosity substrate configurations are utilized. Accordingly, from the simulation, the pressure drop across DOC was observed at 20 mbar for 0.8 liters and 28 mbar for 1.0 liters with 400 cells per square inch (Cpsi) and 4.5 mill-inch wall thickness substrate configurations. Furthermore, the simulated pressure drop across the SCR for a 3.7-litre substrate is 20 mbar. Though the set allowable substrate pressure drop across DOC and SCR is less than 50 mbar, the substrate combination of 0.8 to 1.0 liters of DOC along with a 3.7-litre SCR configuration can be selected for this application.

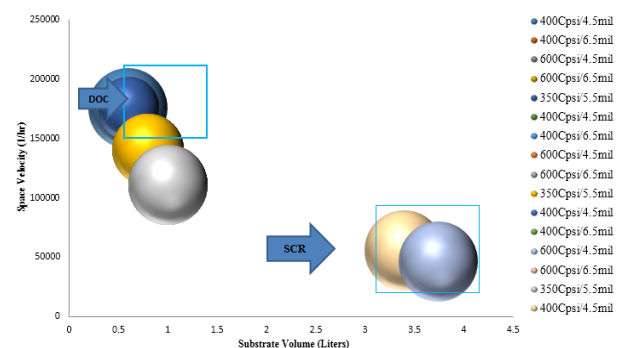


Fig. 11. Space velocity simulation across DOC and SCR substrates

The space velocity simulation across DOC and SCR substrates using the Corning 1D simulator is shown in Figure 11. Usually substrates achieve higher emission conversion for higher space velocities, and this can be accomplished with an increase in substrate volume. Based on the simulation, the observed space velocity is 175300/h-1 for a 0.6 liter, 140200/h-1 for a 0.8 liter, and 110400/h-1 for the given 1.0-litre substrate volumes. However, considering the space velocity target across the DOC (175000/h-1) and SCR (75000/h-1), DOC substrate volumes of 0.8 to 1.0 liter and SCR volumes of 3.4 to 3.7 liters can be preferred. Furthermore, the simulated space velocity for the SCR 3.7-liter substrate is 60000/h-1.

Based on the above simulation results, and the preferred substrate configurations, the modular DOC after-treatment model is designed for 0.8- to 1.0-litre substrates. This model is analyzed for uniformity index analysis using Ansys CFX software. For this flow

analysis, a tetrahedral mesh type was selected. Based on the analysis, it is observed that there are no reverse flow occurrences at the inlet of the cone (DOC inlet). The velocity streamline and contours for the DOC substrate inlet are shown in Figure 12. From the velocity contour, a flow uniformity index of 0.82 is achieved. Though there is a possibility for further cone optimization, considering the impact of DOC system backpressure, this study was carried out with a 0.82 UI design itself.

Testing results:

With the preferred DOC substrate configurations, the emission testing is carried out using a TCIC 27 kW engine (TCIC-Type 2 is engine-out emission without DOC). For this DOC system, the catalyst washcoat combinations are composed of platinum (Pt) and zeolites with an alumina formulation. The zeolite catalyst, with a Si/Al ratio of 5 to 50 and a pore size of about 0.6 nm, is used for trapping diesel HCs at temperatures below about 250 °C and releasing them at temperatures above 250 °C. With the catalyst loading of 1 g/cuft on 0.6 liters of DOC, 0.069 g/kWh (28% reduction) is achieved, 0.8 liters of DOC gives 0.036 g/kWh (62.5% reduction), and 1.0 liters of DOC gives 0.027 g/kWh (71.8% reduction). Overall, the HC conversion efficiency of 1.0-liter DOC with cordierite substrate was higher than that of other DOC volumes. The HC emission performance with DOC is shown in Figure 13.

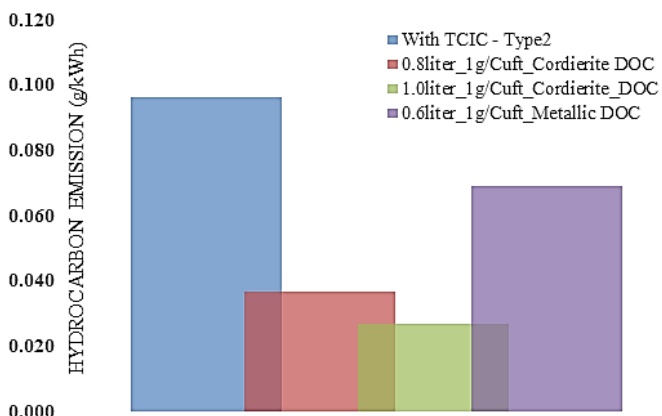


Fig. 12. Velocity streamline and contour for DOC at inlet

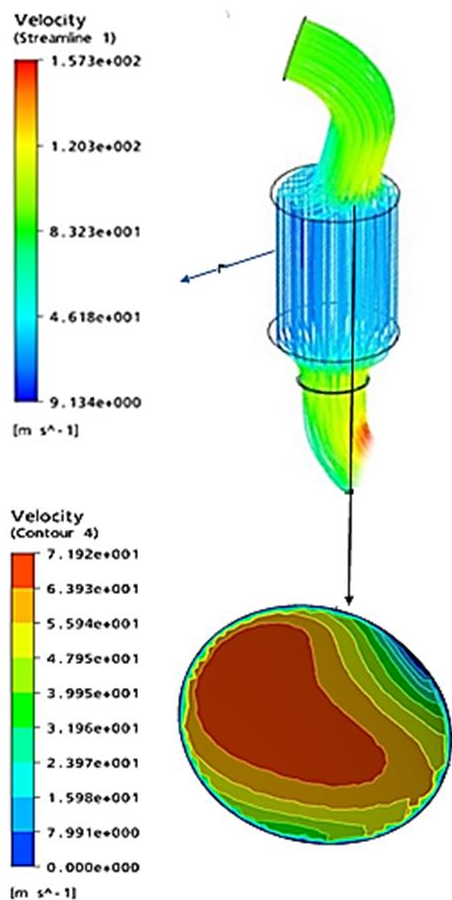


Fig. 13. Hydrocarbon emission with DOC for TCIC engine

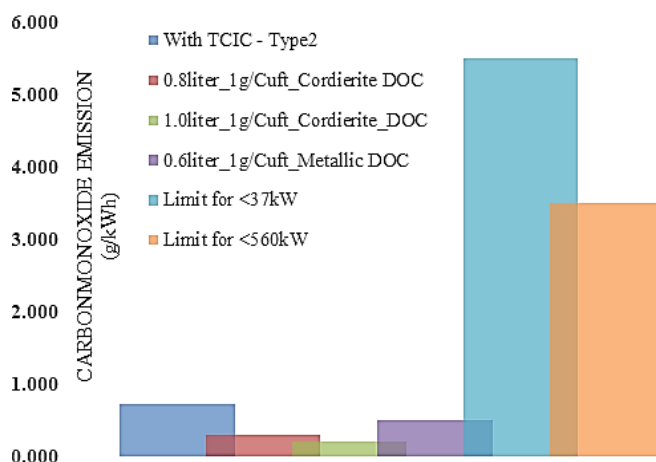


Fig. 14. Carbon monoxide emission with DOC for TCIC engine

Carbon monoxide emission with DOC for the TCIC engine is shown in Figure 14. With a 0.6-litre DOC, 0.497 g/kWh (30% reduction) is achieved. For 1.0-litre DOC, 0.293 g/kWh (59% reduction) and for 0.8-litre DOC, 0.200 g/kWh (43% reduction in CO) are accomplished compared to the TCIC engine without DOC.

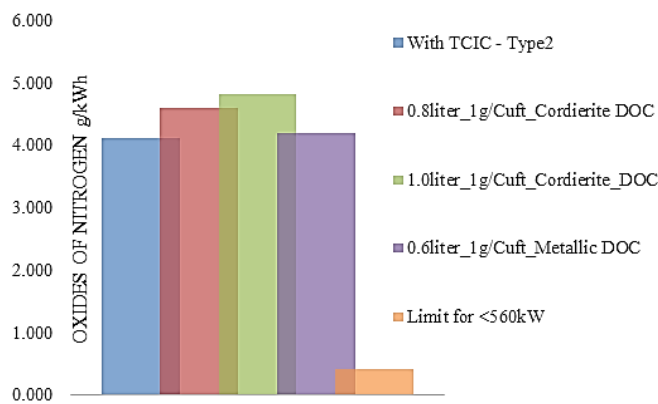


Fig. 15. Oxides of Nitrogen emission with DOC for TCIC engine

The nitrogen oxide emissions with DOC for the TCIC engine are shown in Figure 15. With a 0.6-liter DOC, 4.187 g/kW-h (2.2% increase) is observed. An increase of 11.8% is observed with a 0.8-liter DOC of 4.582 g/kWh. With a 1.0-liter DOC, it produces 4.796 g/kW-h, representing a 17% increase. This shows that NO is being oxidised to NO₂. The 17% NO oxidation will be beneficial for SCR low temperature NO_x conversion as well as DPF passive regeneration.

Simulation results

Figure 16 shows the PM emission simulation for DOC with a TCIC engine using a PM simulator. The PM emission from a 1.0-litre DOC could be 0.22 g/kW-h due to soluble organic fraction oxidation. This still needs further improvement to reduce it below 0.03 g/kW-h. Hence, the need for a DPF system is a must for further soot-related studies.

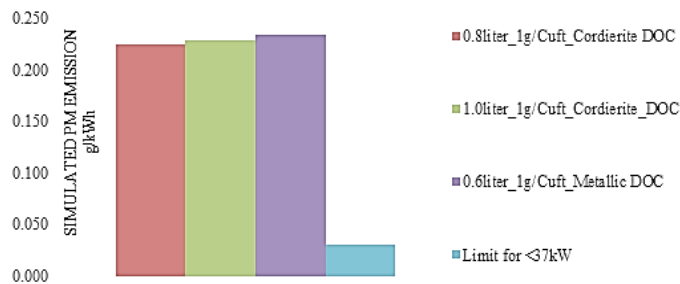


Fig. 16. PM emission simulation with DOC for TCIC engine

Analysis results:

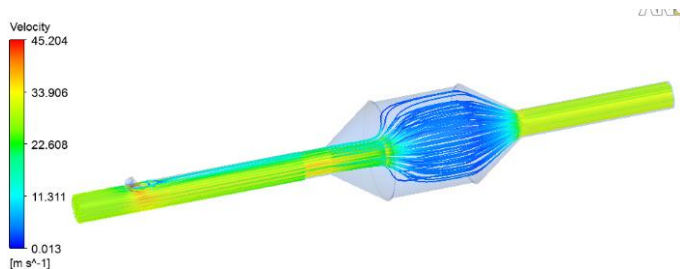


Fig. 17. Velocity contour analysis for SCR using Ansys CFX

Based on the selected substrate configuration, the modular SCR after-treatment system is designed for 3.4-litre and 3.7-litre substrates. This designed model is analyzed for uniformity index using Ansys CFX software. For analysis, the tetrahedral mesh type is selected for this model. Figure 17 shows the velocity contour analysis for SCR using Ansys CFX. It is observed that the inlet to the SCR substrate is without any flow recirculation, and the cone design is well optimized. As an input condition, an inlet exhaust gas mass flow rate of 175 kg/h and an outlet pressure of 1.01325 bar are used, with a linear resistance coefficient of 1072.74 kg/m³s and a quadratic resistance coefficient of 2.749 kg/m⁴.

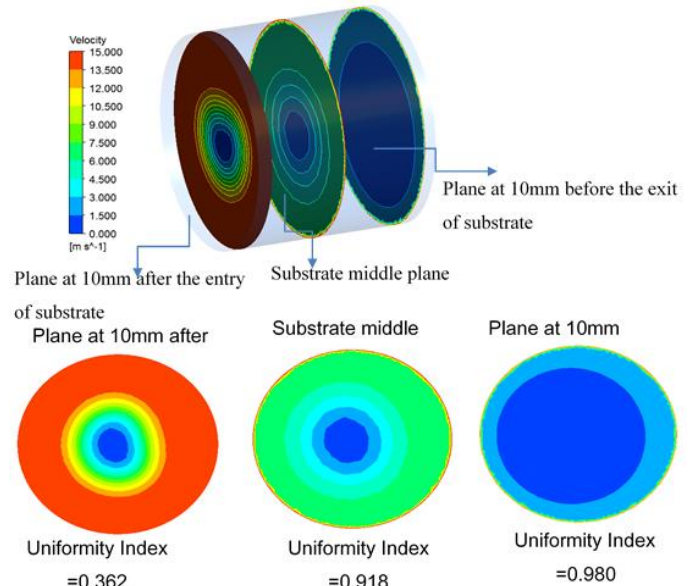


Fig. 18. Uniformity index for SCR using Ansys CFX

Figure 18 shows the uniformity index for SCR using Ansys CFX. According to the analysis, the uniformity index at 10 mm after the cone is 0.362. However, the achieved maximum uniformity index at the substrate middle is 0.918 and at the substrate outlet is 0.9. This shows better mixing of ammonia and exhaust gas before entering the SCR inlet. This could further achieve enhanced NO_x reduction.

GT SUITE Simulation results:

DOC: CO conversion model calibration

CO conversion at 10% and 100% engine load conditions is shown in Figures 19 and 20. CO conversion at 100% load is 91% for the 0.6, 0.8, and 1.0-litre DOC. CO conversion at 10% load is 20% for 0.6 liters, 14% for 0.8 liters, and 30% for 1.0 liters of DOC. The increase in CO conversion efficiency could be due to the selection of DOC with higher space velocity and volume.

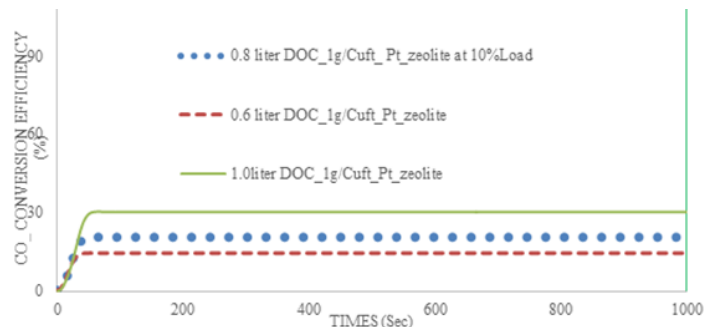


Fig. 19. CO conversion at 10% load using simulation

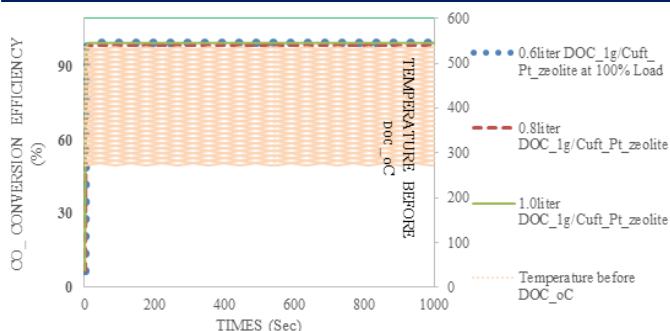


Fig. 20. CO conversion at 100% load using simulation

DOC: HC conversion model calibration

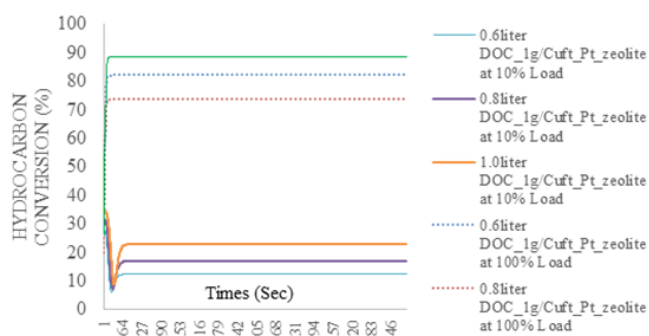


Fig. 21. HC conversion at 10% & 100% using simulation

The HC conversion at 10% and 100% using simulation is shown in Figure 21. At 100% load, 88% HC conversion for 1.0-litre DOC, 82% conversion for 0.8-litre DOC, and 72% HC conversion for 0.6-litre DOC are achieved. At 10% load, HC conversion is 22% for 1.0 litres of DOC, 16% for 0.8 litres of DOC, and 12% for 0.6 litres of DOC. This increase in HC conversion efficiency could be due to the selection of DOC with higher space velocity and volume.

DOC:NO conversion

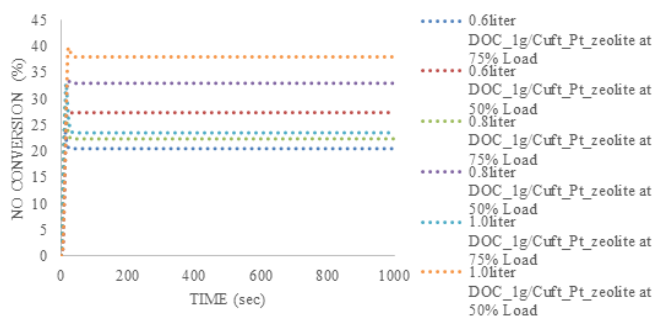


Fig. 22. NO Conversion at 50 & 75% load using simulation

Figure 22 depicts NO conversion at 50% and 75% load using simulation. NO conversion at 50% load provides 37% conversion with 1.0 liters of DOC, 33% conversion with 0.8 liters of DOC, and 27% conversion with 0.6 liters of DOC. These load conditions are selected for simulation based on the NO conversion temperature range. NO conversion at 75% load is 23% for 1.0-litre DOC, 22% for 0.8-litre DOC, and 20% for 0.6-litre DOC. This increase

in NO oxidation to NO₂ could be due to the selection of the DOC with Pt catalyst formulation along with higher space velocity and volume.

HC Conversion: DOC simulation vs. testing comparison

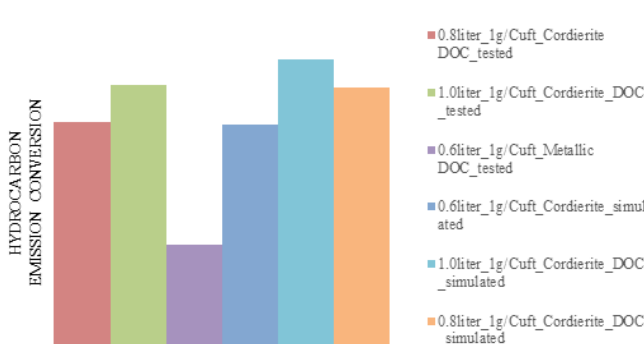


Fig. 23. HC Conversion testing vs. simulation

The DOC:HC conversion for testing versus GT-simulation is shown in Figure 23. The 0.8-litre DOC simulation shows 71% conversion, and the tested results show 62% conversion. Based on simulation, a 1.0-liter DOC achieved 79% HC conversion, while tested results show 72% conversion. The overall difference between simulation and tested results is in the range of 8–12% for 1.0-litre DOC; this difference is carried out for SCR calibration purposes.

CO conversion: DOC simulation vs. testing comparison

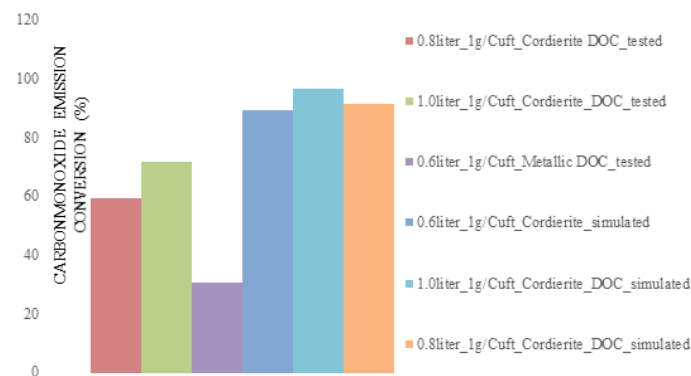


Fig. 24. CO conversion: actual vs. simulation

The CO conversion for testing versus GT-simulation is shown in Figure 24. For a 0.8-litre simulation, results show 91% conversion, and tested results show 59%. Simulation results show 96% conversion, while tested results show 72% conversion for 1.0-liter DOC. The observed difference between simulation and testing results is 25%. This difference is carried out for SCR calibration purposes. However, this difference could be due to a de-greening effect, which is not considered during simulation. Furthermore, fuel with a sulphur content of 50 ppm is used during testing, and this could also cause variations in catalyst performance during testing and simulation.

NOx conversion and ammonia slip simulation with 3.4-litre SCR

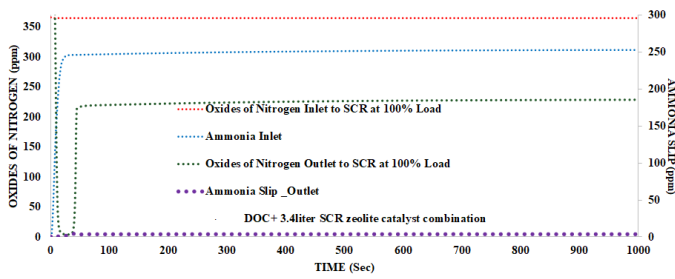


Fig. 25. NOx conversion and ammonia slip with 3.4-litre SCR at 100 % load

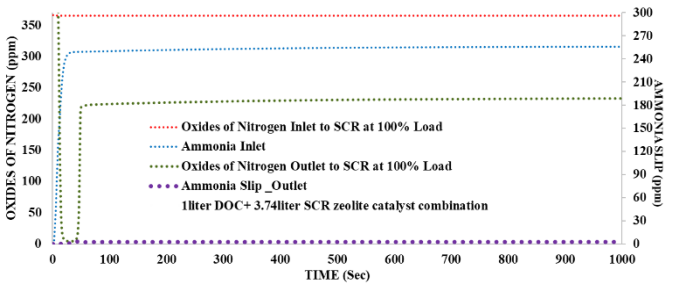


Fig. 26. NOx conversion and ammonia slip with 3.7-litre SCR at 100 % load

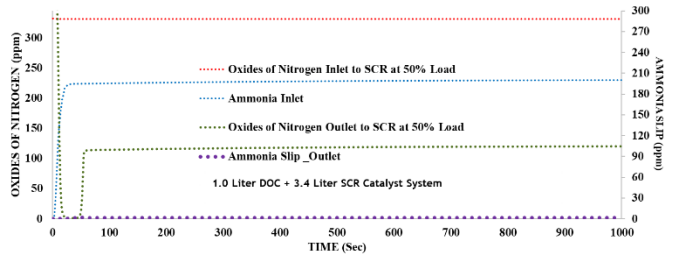


Fig. 27. NOx conversion and ammonia slip with 3.4-litre SCR at 50 % load

Figures 25 and 26 show a GT-simulation of NOx conversion with 3.4 and 3.7 liters of SCR substrate volume, respectively. This simulation is carried out at an ammonia-to-NOx ratio of 1 (ANR = 1). This condition is maintained to keep the slip at a lower level. At 100% load, 49% NOx conversion and an ammonia slip of 3 ppm for a 3.4-litre SCR system are observed. Furthermore, for the same load condition, the observed NOx conversion with 3.7-liter SCR substrate is >48% with an ammonia slip of 2.7 ppm.

Figures 27 and 28 show NOx conversion simulations with a 3.4- and 3.7-liter-volume SCR substrate at 50% load. With a 3.4-litre SCR system, NOx conversion is > 46% with an ammonia slip of 3 ppm. NOx conversion is greater than 55% with a 3.7-liter SCR substrate, and ammonia slip is less than 2.7 ppm. It shows the ammonia-to-NOx ratio maintained at ANR = 1 can reduce the ammonia slip to a lower level.

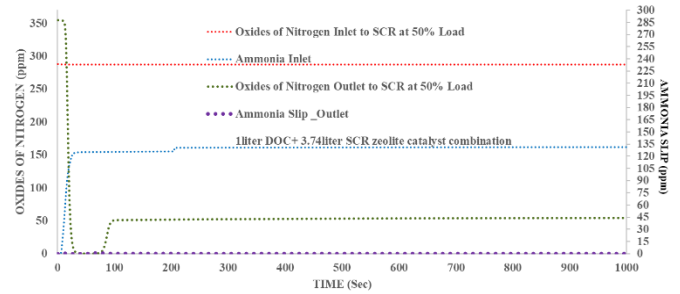


Fig. 28. NOx conversion and ammonia slip for 3.7-litre SCR at 50 % load

DPF pressure drop simulation at 'o'gms soot condition

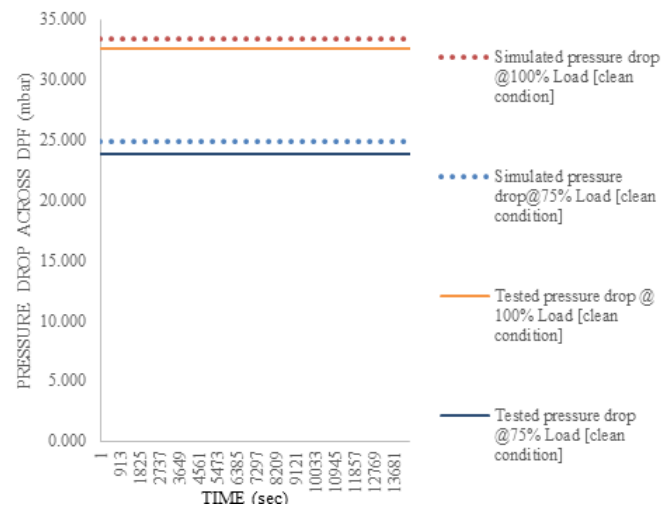


Fig. 29. Pressure drop at 'o'g soot condition using simulation

Figure 29 shows the pressure drop in clean condition across the DPF. The maximum pressure drop across the DPF for a clean condition (without soot) at 100% load is 33 mbar. Further, the DPF model is calibrated with tested results to establish correlations for simulated results within 2% of variations. Further, emission outputs from DOC and SCR are used as the input for the DPF, considering the NO2 generation out of SCR is used to oxidise the soot. Inside the DPF, the soot particles are filtered and retained due to surface filtration along the channel walls as well as depth filtration inside the filter pores. This process is called soot cake formation. Hence, during cake formation, a small fraction of the soot initially collects in the filter pores and then consequently builds a layer on the DPF channel walls laterally. This accumulated soot provides an additional layer to trap further incoming particles. This can be confirmed by observing a consistent pressure drop after running the engine continuously for an extended period of time (> 2.5 hours) or after degreening. Figure 30 (a) shows the pressure drop vs. soot load simulation at 100% load. During this condition, 7.6 g of soot accumulated and a pressure drop of 136 mbar across the DPF was observed. Figure 30 (b) shows 7.0 g of soot accumulation at 75% load with a pressure drop of 101 mbar across the DPF. Figure 30 (c) shows 6.0 g of soot accumulation at 50% load with a pressure drop of 67 mbar across the DPF. Figure 30 (d) shows 4.2 g of

soot accumulation at 10% load with a pressure drop of 26 mbar across the DPF.

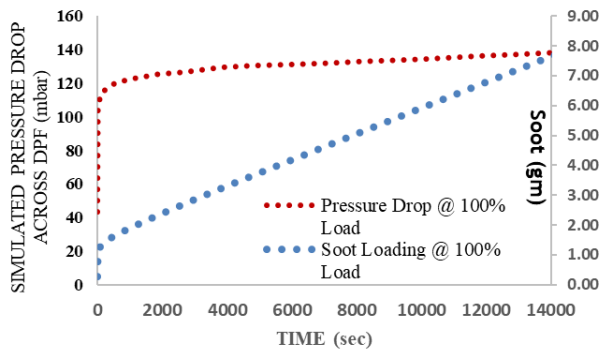


Fig. 30 (a). Pressure drop vs soot load simulation at 100% load

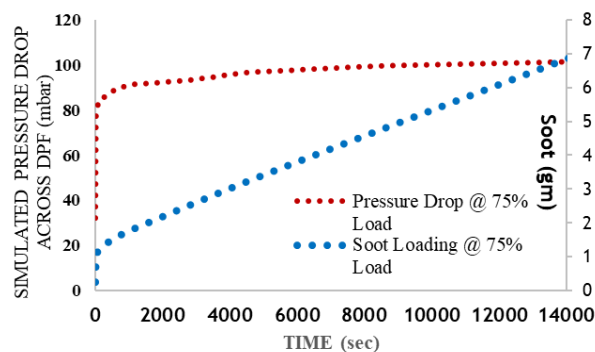


Fig. 30 (b). Pressure drop vs soot load simulation at 75% load

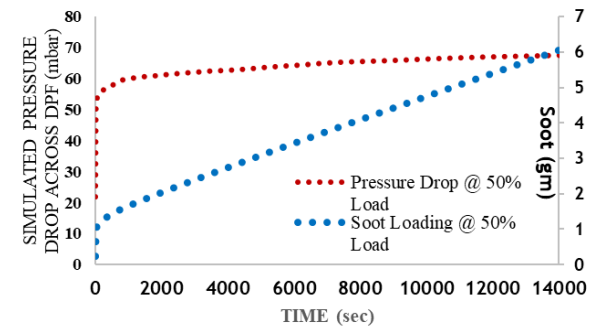


Fig. 30 (c). Pressure drop vs soot load simulation at 50% load

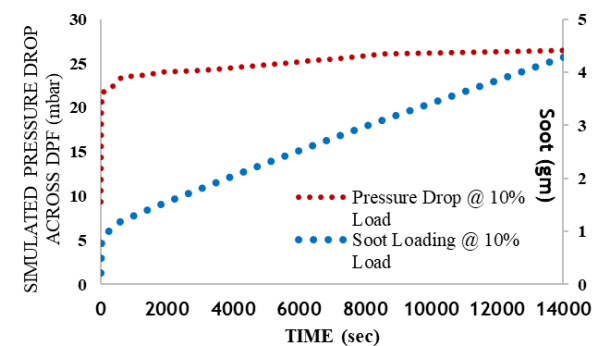


Fig. 30 (d). Pressure drop vs soot load simulation at 10% load

Regeneration time and ash formation simulation with 8gm soot condition

Regeneration time and ash formation with 8 g of soot are shown in Figure 31. For a 538 oC DPF (4.7-litre DPF) inlet temperature, the regeneration time for 8 g of soot loading is less than 57 seconds at 100% load. This regeneration time interval typically depends on the exhaust gas temperature.

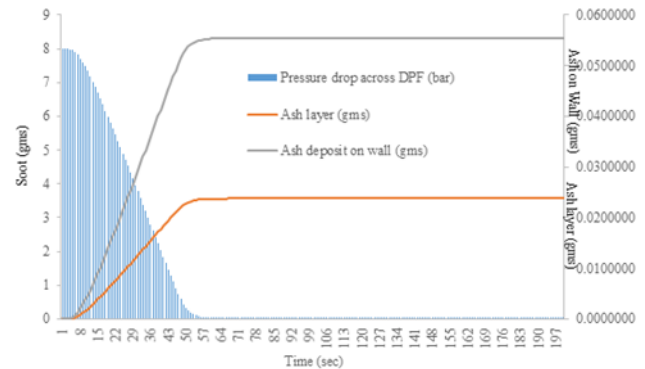


Fig. 31. Regeneration time and ash formation with 8gm soot

Furthermore, 0.07 g of ash is generated during the regeneration of 8 g of soot.

Regeneration time comparison for 50 to 100 % load

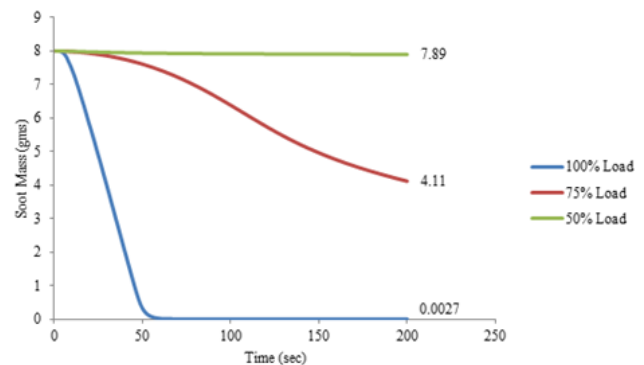


Fig. 32. Regeneration time comparison for 100%, 75%, 50% load

Soot regeneration time comparisons for 100%, 75%, and 50% load are shown in Figure 32. At a 100% load condition, the soot regeneration time is 50–60 sec. Further, for 100% and 75% load conditions, the observed DPF regeneration temperature is favourable. However, temperature conditions below 50% load are unfavourable for regeneration. As a result, thermal insulation before the DPF inlet is required to improve further and reduce regeneration time.

Heat insulation testing results:

The Nanox coating thermal insulation performance on DOC is shown in Figure 33. Without this Nanox coating on the DOC outer shell, the DOC's out temperature is 538 oC at 100% load, and it gets reduced to 523oC. As a result, the temperature dropped by

150C after DOC. However, with the Nanox coating of 500 μ m, on DOC outer shell, the temperature further improved to 529oC. This shows a 4-6oC improvement. Accordingly, further to reduce this temperature loss, insulation required from the exhaust manifold to DOC and this can enhance thermal retention before DPF to maintain the favourable temperature conditions for soot regeneration.

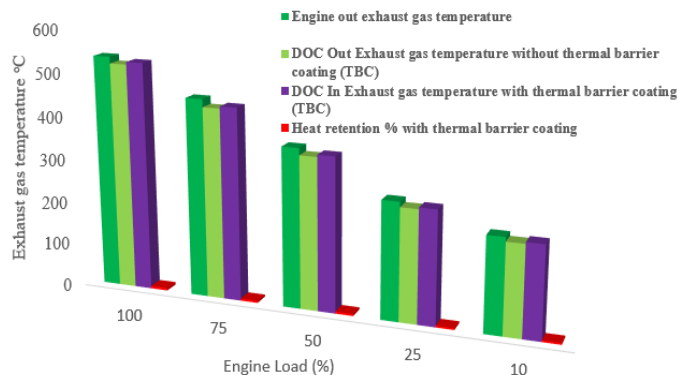


Fig. 33. Nanox coated DOC thermal insulation performance.

In this investigation, 7% wt YPSZ (Nanox) is coated on the DOC (external surface) of the outer shell using Nanox S4007 powder and coating plasma spray technology. The Y2O3-ZeO2 weight ratio is 7:93, and the agglomerated powder size of 15–150 microns is used for this study.

3. Conclusions

From the present investigations, the following conclusions are drawn:

DOC with 1.0-liter substrate volume and 1 g/cuft shows HC conversion of 72% (HC mass emission is 0.027 g/kWh), which is favourable for meeting proposed emission norms. CO conversion is 73% (mass emission is 0.200 g/kWh). Further, the achieved emission limit (HC: 0.027 + NOx: 4.13) is within the mass emission limit of 4.7 g/kWh norms. With a 3.7-liter SCR catalyst, NOx is further reduced by 75% with 3 ppm NH3 slip, achieved using GT-SUITE simulation. This could be beneficial for meeting future NOx emission norms as well.

Further, with this TCIC engine along with the 1.0-litre DOC system, the smoke values are measured to simulate the PM using the AVL soot calculator model. The simulated value is 0.22 g/kWh, and this requires further reduction in PM. Based on the GT-SUITE simulation technique for further PM reduction, favourable regeneration conditions were simulated. Based on this simulation study, the maximum soot mass limit of 8 gm is simulated for the selected 4.7-liter DPF. Furthermore, the simulated temperature ranges between 450 and 550 oC are favourable for active regeneration at 75% and 100% load conditions. However, for the load ranges below 50%, temperature improvement for regeneration is required. As part of DPF temperature improvement, an advanced Nanox (7% YPSZ) coating is provided on the DOC outer shell (Nanox top coat layer of 460–480 microns) and tested. At rated load conditions, a maximum of 6 oC temperature improvement is accomplished at the inlet of the DPF. However, if this Nanox coating is applied over

the exhaust manifold itself, then further temperature enhancement in the DPF inlet could be achieved. Overall, in this study for diesel engines ranging between 19 and 27 kW, it is demonstrated that with the appropriate selection of after-treatment system design, catalyst material, and substrate configurations, proposed emission limits can be accomplished.

Acknowledgment

The authors would like to thank BASF Catalyst India for after-treatment system development. Additionally, the authors would like to thank Dr. Aruna, Scientist, Coatings Division, National Aerospace Laboratory, Bangalore, India, for providing the coating facility for this research activity.

Nomenclature

DOC	: Diesel oxidation catalyst
DPF	: Diesel Particulate Filter
SCR	: Selective Catalytic Reduction
TCIC	: Turbocharged intercooled
PM	: Particulate matter

Conflict of Interest Statement

The authors declare that there is no conflict of interest in the study.

CRediT Author Statement

Annamalai Kandaswamy: Conceptualization, Supervision,
Karthikeyan Subramanian: Conceptualization, Writing-original draft, Validation, Data collection, Formal analysis.

References

- [1] Tyagi, N., gupta, S., Bhardwaj, P., Gayen, H. Vijayakumar Thulasi. Optimization of GENSET Engine for CPCB- II Norms using Cost Effective Techniques. SAE Technical Paper 2013-01-2838, 2013, <https://doi.org/10.4271/2013-01-2838>.
- [2] Issa, M., Ibrahim, H., Lepage, R. and Ilinca, A. A Review and Comparison on Recent Optimization Methodologies for Diesel Engines and Diesel Power Generators, Journal of Power and Energy Engineering, 7, 31-56; [doi: 10.4236/jpee.2019.76003](https://doi.org/10.4236/jpee.2019.76003).
- [3] Karthikeyan.S, Suresh. A. L, Sathyanadan. M, Krishnan.S, Sh-Iavan Kumar Srisailam and Weiyong Tang. Performance of BS-VI catalyst and influence of deactivation conditions on emission durability for commercial vehicle applications. Materials today: Proceedings; 2022; <https://doi.org/10.1016/j.matpr.2022.09.564>.
- [4] Karthikeyan.S, Suresh. A. L, Sathyanadan. And Mahesh. P. A competent top down approach methodology for design and development of commercial vehicle box type exhaust after treatment system. Materials today: Proceeding; 2022. <https://doi.org/10.1016/j.matpr.2022.08.556>.
- [5] Hirose, S., Miyairi, Y., Katsube, F., Yuuki, K. Hirofumi Sakamoto, Claus Vogt, Shuji Fujii. Newly Developed Cordierite Honeycomb Substrate for SCR Coating Realizing System Compactness and Low Backpressure. SAE Technical Paper 2012-01-1079, 2012, <https://doi.org/10.4271/2012-01-1079>.

- [6] Karthikeyan, S., Annamalai, K. Study on Performance Enhancement Technologies for Two Cylinder Diesel Engine for Off-Road Applications. In: Narasimhan, N.L., Bourouis, M., Raghavan, V. Recent Advances in Energy Technologies. Lecture Notes in Mechanical Engineering. Springer, Singapore; 2023 https://doi.org/10.1007/978-981-19-3467-4_37
- [7] Harne, P., Dhamangaonkar, P., and Kalaiselvan, K. Performance Assessment of Urea-Selective Catalytic Reduction (SCR) Technology in On-Road 6-Cylinder Heavy-Duty Diesel Engine. SAE Technical Paper 2020-28-0324, 2020; <https://doi.org/10.4271/2020-28-0324>.
- [8] Hirose, S., H. Yamamoto, H. Suenobu, H. Sakamoto, F. Katsube, P. Busch, A. Martin, R. Kai, and C. D. Vogt. Development of High Porosity Cordierite Honeycomb Substrate for SCR Application to Realize High NOx Conversion Efficiency and System Compactness. SAE International Journal of Materials and Manufacturing. 2014;7(3). <http://www.jstor.org/stable/26268654>.
- [9] De Rudder, K., Tier 4 High Efficiency SCR for Agricultural Applications, SAE Int. J. Commercial. Veh. 2012;5(1):386-394. <https://doi.org/10.4271/2012-01-1087>.
- [10] Kiminobu Hirata, Nobuhiko Masaki, Hiroki Ueno and Hisashi Akagawa. Development of urea SCR system for Heavy –Duty Commercial vehicles. SAE Technical Paper 2005-0-1860; <https://doi.org/10.4271/2005-01-1860>.
- [11] Subramanian, K., A, S., Mahadevan, S., and Sadagopan, K. Emission Performance and Durability Validation Methodology for Heavy Commercial Vehicle After-treatment Systems. SAE Technical Paper 2022-28-0327; 2022. <https://doi.org/10.4271/2022-28-0327>.
- [12] S. Karthikeyan, K. Annamalai and M. Sathyanandan. Diesel engine performance improvement with suitable low cost technologies for tractor applications. Progress in Industrial Ecology, An International Journal; 2015. <https://doi.org/10.1504/PIE.2015.073087>.
- [13] Karthikeyan, S and Annamalai. Study on Exhaust Emission Performance with advanced after-treatment systems for two-cylinder diesel engine, 4th International conference on advances in mechanical engineering; India, 2022.
- [14] Niemi, S., Laurén, M., and Murtonen, T. Effect of Waste-Gate Turbocharging on the Exhaust Particulate Matter of an Off-Road Diesel Engine. SAE Technical Paper 2002-01-2159, 2002; <https://doi.org/10.4271/2002-01-2159>.
- [15] Zagade, B., Sharma, V., and Körfer, T, Tuning and Validation of DPF for India Market. SAE Technical Paper 2017-26-0135, 2017; <https://doi.org/10.4271/2017-26-0135>.
- [16] Iwasaki, S., Mizutani, T., Miyairi, Y., Yuuki, K. et al. New Design Concept for Diesel Particulate Filter. SAE Int. J. Engines. 2011;4(1):527-536. <https://doi.org/10.4271/2011-01-0603>.
- [17] Nishioka, A., Sukegawa, Y., Katogi, K., Mamada, H., Takehiko Kowatari, Toshifumi Mukai, Hiroshi Yokota. A Study of a New Aftertreatment System (2): Control of Urea Solution Spray for Urea-SCR. SAE Technical Paper 2006-01-0644, 2006; <https://doi.org/10.4271/2006-01-0644>.